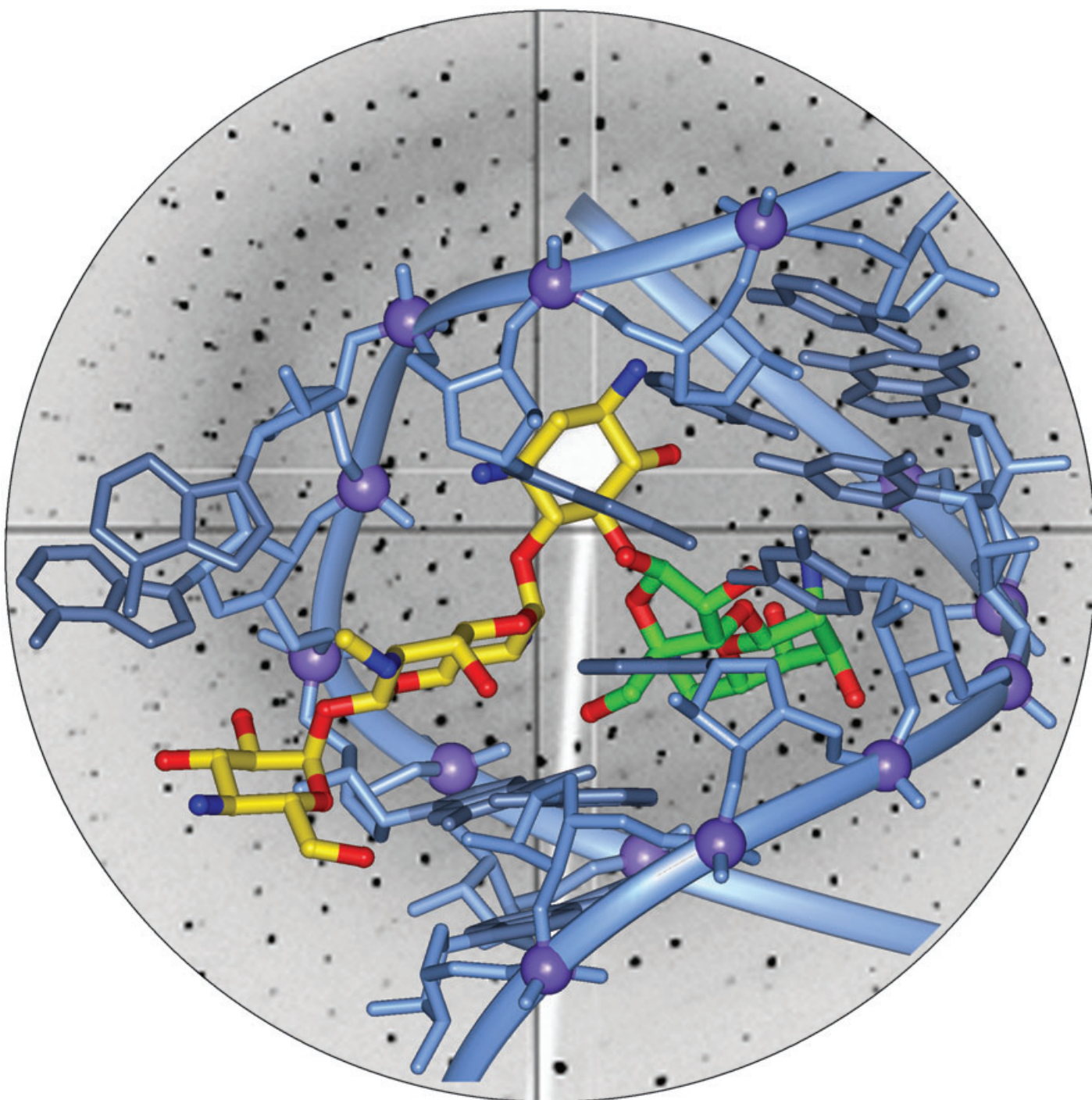


# Communications



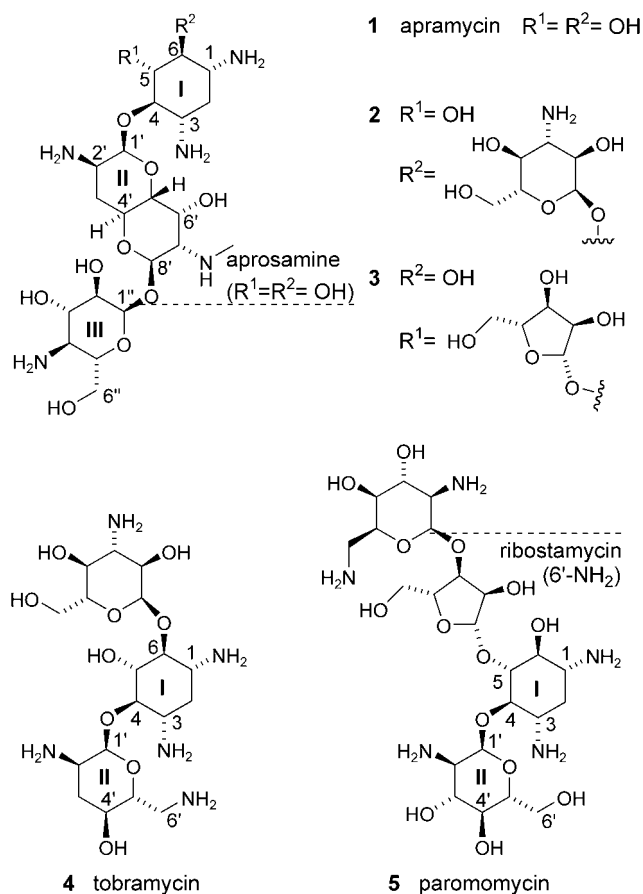
The aminoglycosides apramycin (yellow) and paromomycin (green) exploit different binding spaces at their target ribosomal decoding-site RNA although they share a common 2-deoxystreptamine scaffold (white center). More about these studies on molecular recognition can be found in the Communication by T. Hermann and co-workers on the following pages.

## Molecular Recognition by Glycoside Pseudo Base Pairs and Triples in an Apramycin–RNA Complex\*\*

Qing Han, Qiang Zhao, Sarah Fish, Klaus B. Simonsen, Dionisios Vourloumis, Jamie M. Froelich, Daniel Wall, and Thomas Hermann\*

The ribosome and its RNA components are targets for a diverse set of antibiotics, including the natural aminoglycosides, macrolides, and tetracyclins and the synthetic oxazolidinones, all of which interfere with bacterial protein synthesis.<sup>[1,2]</sup> Crystallographic analyses of ribosomal subunits and domains thereof in complex with antibiotics have demonstrated that the natural products interact almost exclusively with ribosomal RNA components (rRNA),<sup>[3]</sup> a result that lends support to earlier biochemical findings<sup>[4,5]</sup> and underlines the importance of RNA as a drug target.<sup>[6]</sup> Aminoglycoside antibiotics bind to 16S rRNA near the mRNA decoding site and thereby decrease the fidelity of translation by lowering the energetic cost of a conformational transition in the ribosome that is required for the discrimination between near-cognate and cognate tRNAs.<sup>[7,8]</sup> Insight into the molecular recognition of the decoding site by antibiotic ligands and the mechanics of translational fidelity are emerging from three-dimensional structures of aminoglycosides in complex with decoding-site oligonucleotides and whole 30S ribosomal subunits.<sup>[7,9–13]</sup>

Crystal structures have been determined for RNA complexed with two classes of aminoglycosides (Scheme 1). The three-dimensional structures of paromomycin (**5**) as well as tobramycin (**4**) and geneticin bound to the whole 30S ribosomal subunit and to small model oligonucleotides revealed a key role for the 2-deoxystreptamine (2-DOS) moiety in RNA recognition.<sup>[10–12,14]</sup> In all cases, the 2-DOS ring interacts with two consecutive base pairs of the decoding-site RNA, that is, C1407–G1494 and the non-Watson–Crick pair



**Scheme 1.** Aminoglycoside antibiotics that bind to the bacterial decoding-site RNA. Apramycin (**1**), a unique 4-monosubstituted 2-deoxystreptamine, is described herein. Compounds **2** and **3** are semisynthetic apramycin derivatives.<sup>[35]</sup> Aprosamine is obtained from apramycin by acid hydrolysis of the terminal sugar (III) to leave a free hydroxy group at the 8'-position.<sup>[15]</sup> Crystal structures of decoding-site RNA complexed with tobramycin (**4**), a 4,6-disubstituted 2-deoxystreptamine, and paromomycin (**5**), a 4,5-disubstituted 2-deoxystreptamine, were described recently.<sup>[7,9–11]</sup> The 2-deoxystreptamine moiety shared by all structures is numbered I. The ring fragments numbered II are derived from glucose.

U1406○U1495 (Figure 1 a). Since these base pairs are conserved in both the bacterial and eukaryotic decoding site, molecular discrimination of the bacterial target by aminoglycosides is provided through a combination of sugar substituents at the 4- and 5- or the 4- and 6-positions of the 2-DOS moiety.

Apramycin (**1**) is unique among the aminoglycosides as it achieves antibacterial specificity by sugar substitution of the 2-DOS ring at the 4-position only (Scheme 1).<sup>[15–17]</sup> Chemical probing has been used to study binding of apramycin to the bacterial decoding site and has revealed specific interactions of the antibiotic with residues A 1408 and G 1494,<sup>[5]</sup> which also participate in the binding of the 4,5- and 4,6-disubstituted 2-DOS compounds.<sup>[10–12,14]</sup> In contrast to these aminoglycosides, which induce miscoding during translation, the primary effect of apramycin is inhibition of elongation by blocking ribosome translocation.<sup>[17]</sup> To decipher the molecular recognition of the bacterial rRNA target by apramycin, we have determined by

[\*] Dr. Q. Han, Dr. Q. Zhao, S. Fish, Dr. T. Hermann  
 Department of Structural Chemistry  
 Anadys Pharmaceuticals, Inc.  
 3115 Merryfield Row, San Diego, CA 92121 (USA)  
 Fax: (+1) 858-527-1539  
 E-mail: thermann@anadyspharma.com

Dr. K. B. Simonsen,<sup>†</sup> Dr. D. Vourloumis  
 Department of Medicinal Chemistry  
 Anadys Pharmaceuticals, Inc. (USA)

J. M. Froelich, Dr. D. Wall  
 Department of Microbiology  
 Anadys Pharmaceuticals, Inc. (USA)

[<sup>†</sup>] Current address:  
 H. Lundbeck A/S  
 Copenhagen Valby (Denmark)

[\*\*] This work was supported by the National Institutes of Health (Grant no. AI51104 to T.H.).

Supporting Information for this article is available on the WWW under <http://www.angewandte.org> or from the author.



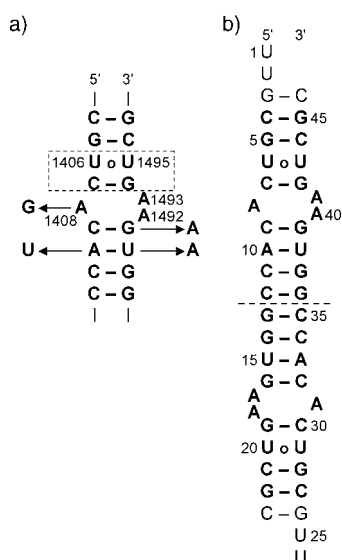


**Figure 1.** a) Secondary structure of the bacterial decoding-site internal loop in 16S rRNA. The four base changes of the eukaryotic sequence are indicated by arrows. The recognition site for the 2-DOS moiety of aminoglycosides is boxed. b) RNA construct used for cocrystallization with apramycin. Due to the self-complementarity of the single strands, two antiparallel decoding-site loops are formed. Residues that are specific to the bacterial decoding site are shown in bold.

X-ray crystallography the three-dimensional structure of apramycin complexed to the bacterial decoding site in an RNA model construct (Figure 1 b). Similar constructs have been used before for crystallographic structure determination of aminoglycoside–RNA complexes and were proved to represent authentic models of the ribosomal decoding site.<sup>[10–12,14,18]</sup>

In the crystal structure of the apramycin–RNA complex, both decoding-site internal loops are occupied by the aminoglycoside (see the Supporting Information). One of the ligand-binding sites participates in crystal-packing contacts, involving A 1492 and A 1493 in an interdigitated stacking arrangement with a neighboring RNA molecule, while the other decoding site is unperturbed by intermolecular contacts. As the geometry of the two ligand-binding sites is similar, we focus here on the analysis of the unperturbed site (Figure 2). The overall structure of the internal-loop RNA resembles the decoding-site complexes of paromomycin, tobramycin, and geneticin that were previously described.<sup>[10–12,14]</sup> The unpaired A 1408 residue is stacking between flanking base pairs and interacting with apra-

mycin which spans the RNA helix from the interior at the deep (major) groove to the exterior at the shallow (minor) groove. The A 1492 and A 1493 residues are flipped out from the interior of the RNA helix, thereby creating an opening that accommodates the aminoglycoside (Figure 2 a).

The C 1407–G 1494 base pair and the U 1406⊙U 1495 non-Watson–Crick pair form both direct and water-mediated hydrogen bonds with the 2-DOS ring (I) of apramycin (Scheme 2 a). The hydrogen-bonding pattern and position of the apramycin 2-DOS ring relative to the RNA are similar to those of the 2-DOS moiety in the decoding-site complexes of other aminoglycosides (Figure 2 b and c).<sup>[10–12,14]</sup> The geometry of the U 1406⊙U 1495 pair most closely resembles the structure of this pair in the geneticin complex,<sup>[14]</sup> but with a relative translation of the residues that results in compression of the RNA helix diameter (9.3 Å C1'–C1' distance, in comparison with 9.8 Å in the geneticin complex). It has been pointed out that a U 1406A change confers resistance specifically to the 4,6-disubstituted 2-DOS aminoglycosides whose sugar substituent at the 6-position cannot be accommodated when a A 1406–U 1495 pair is present.<sup>[18]</sup> Apramycin, which does not carry substituents at either the 5- or 6-positions, can still bind to the U 1406A decoding-site mutant. The 2-DOS interaction pattern in the apramycin complex is in agreement with susceptibility data for bacteria carrying a U 1406A mutation, which show a fourfold hypersensitivity to this antibiotic.<sup>[19]</sup> Molecular modeling of an A 1406–U 1495

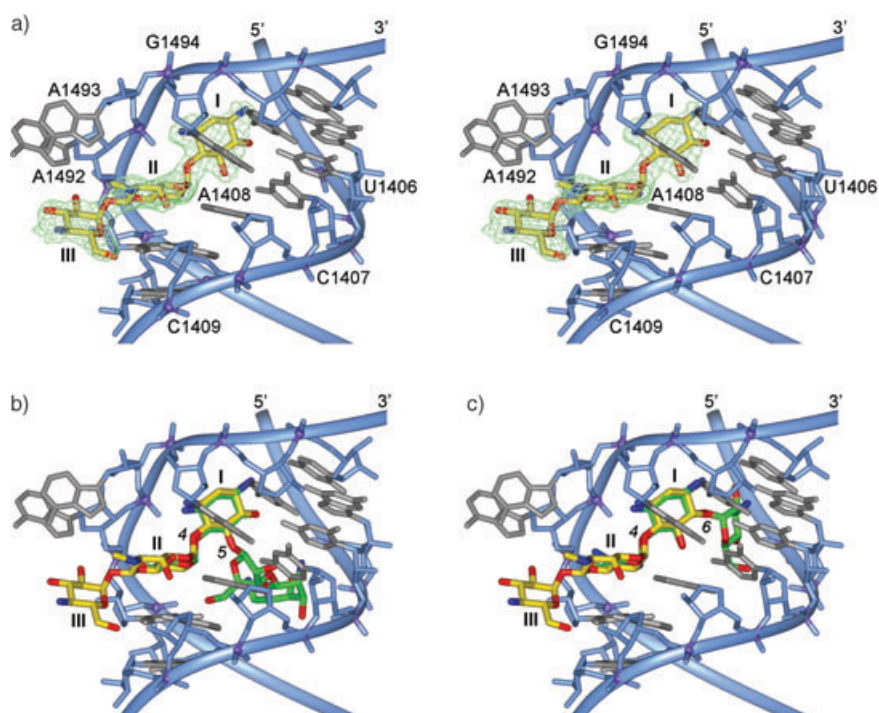
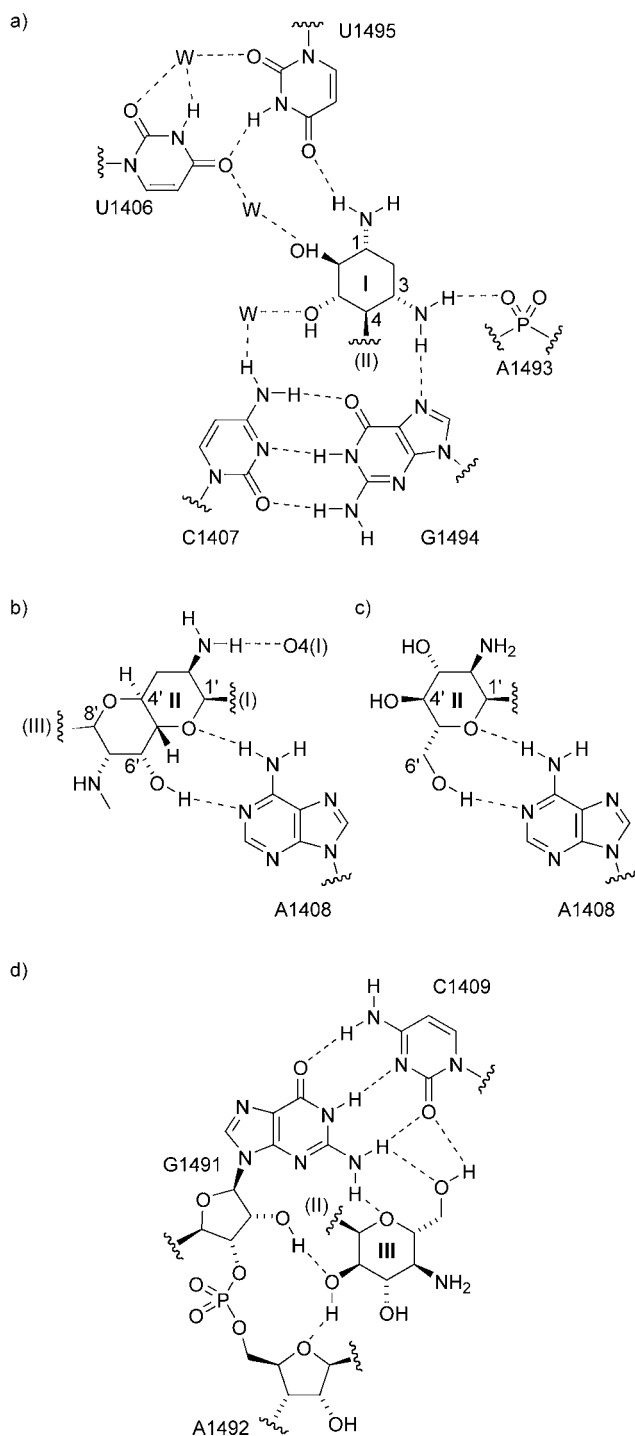


**Figure 2.** a) Stereoview of the apramycin–decoding-site RNA complex. Electron density ( $2F_o - F_c$ ) is contoured at  $1.0\sigma$  around the aminoglycoside. Apramycin (yellow) ring fragments are numbered according to the sequence shown in Scheme 1. b) Superimposition (based on phosphate coordinates) of the complexes of apramycin (yellow) and paromomycin<sup>[10]</sup> (green) with the decoding site. Only the RNA of the apramycin complex is shown. The 4- and 5-substitution positions of the 2-DOS core in paromomycin are indicated. c) Superimposition (based on phosphate coordinates) of the complexes of apramycin (yellow) and tobramycin<sup>[11]</sup> (green) with the decoding site. The 4- and 6-substitution positions of the 2-DOS core in tobramycin are indicated. Base numbering follows the *Escherichia coli* sequence (see Figure 1).



**Scheme 2.** a) Hydrogen-bonding interactions of the apramycin 2-DOS moiety with the decoding-site RNA target. Water molecules are indicated as W. b) Base-pair-like interaction of the bicyclic sugar (II) of apramycin with the A1408 residue. This can be compared with c) the interaction of the glucosamine moiety (II) of paromomycin with A1408.<sup>[10]</sup> d) Base-triple-like docking of the terminal sugar fragment (III) of apramycin to the minor-groove edge of a G–C pair. Base numbering follows the *Escherichia coli* sequence (see Figure 1).

Watson–Crick pair in the decoding-site structure shows that a water-mediated hydrogen bond could be formed between the 6-hydroxy group of the 2-DOS ring and the 4-amino

substituent of A1406. This water-mediated interaction would adopt a more favorable geometry than the observed contact between the same 2-DOS hydroxy group and O4 of U1406 in the apramycin–wild-type RNA complex. Similar observations have been made for paromomycin and neomycin B,<sup>[19]</sup> 4,5-disubstituted 2-DOS aminoglycosides whose binding to the decoding site is positively affected by the U1406A mutation.<sup>[18]</sup>

The bicyclic sugar (II) of apramycin is stacking over the guanine base of the C1409–G1491 pair (Figure 2), aligned in a coplanar manner, and forming direct hydrogen-bond interactions with the A1408 residue (Scheme 2b). The ring connected to the 2-DOS moiety is located in a position similar to that of the glucosamine residue in other aminoglycosides bound to the decoding-site RNA (Figure 2b and c).<sup>[10–12,14]</sup> The hydrogen-bonding pattern between O1' and O6' of the apramycin sugar (II) and A1408 is identical to the interactions seen for the glucosamine ring in the paromomycin complex (Scheme 2c), and it gives rise to a geometry that has been described as a glycoside–adenine pseudo base pair.<sup>[14]</sup> The 2'-amino group of apramycin is involved in an intramolecular contact to O5 of the 2-DOS moiety. The interaction between the bicyclic sugar (II) of apramycin and A1408 explains susceptibility data for bacteria carrying an A1408G mutation or a methylated A1408 residue, either of which confers resistance to apramycin.<sup>[20,21]</sup> Methylation of the adenine exocyclic amino group or change to a guanine at residue 1408 prevents formation of the glycoside pseudo base pair with the apramycin sugar (II).

The terminal sugar (III) of apramycin is aligned at the shallow-groove edge of the C1409–G1491 pair and forms two direct hydrogen bonds to these bases, thereby resulting in an interaction that we termed a glycoside pseudo base triple (Scheme 2d). The geometry of the interaction closely resembles the arrangement of shallow-groove X–G–C base triples that occur in ribosomal RNA, such as the G2588–G2617–C2542 triple in 23S rRNA from *Haloarcula marismortui* and the A1085–G1055–C1104 triple in 23S rRNA from *Escherichia coli* (see also Figure S2 in the Supporting Information).<sup>[22,23]</sup> Shallow-groove recognition of RNA base pairs has frequently been observed in protein–RNA complexes, such as the ribosome, spliceosomal particles, and aminoacyl-tRNA synthetases.<sup>[24]</sup>

The 6''-hydroxy group of apramycin that participates in the interaction with the C1409–G1491 pair is located at a position that is occupied by a water molecule in the decoding-site complexes of tobramycin and geneticin.<sup>[11,12]</sup> Additional hydrogen bonds are formed between the 2''-hydroxy substituent of apramycin and the ribose moieties of G1491 and A1492. Apramycin, which lacks the terminal sugar (III) of apramycin (Scheme 1),<sup>[15]</sup> still binds to the bacterial decoding-site RNA, albeit with a lower affinity that leads to a tenfold loss of potency in translation inhibition and bacterial growth suppression.<sup>[25]</sup> The interaction between the apramycin terminal sugar (III) and the C1409–G1491 pair is in agreement with bacterial resistance conferred by decoding-site mutations at these residues. Earlier investigations of *E. coli* strains carrying all possible nonlethal single and double mutations at the 1409 and 1491 residue positions showed that any change

of the wild-type C–G pair results in 2- to 64-fold decrease in susceptibility to apramycin.<sup>[26]</sup>

Superimposition of the apramycin–RNA complex with the crystal structure of the 30S ribosomal paromomycin complex<sup>[7]</sup> shows that the orientation of the apramycin sugar (III) projects the 3'-hydroxy group into close proximity (<2 Å) with the T40 residue of ribosomal protein S12 (Figure 3). Recent functional studies of S12 have revealed

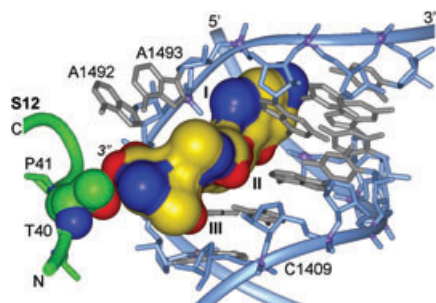


**Figure 3.** Superimposition (based on phosphate coordinates) of the apramycin–RNA complex with the decoding site in the crystal structure of the whole 30S ribosomal subunit complex with paromomycin.<sup>[7]</sup> The molecular surface of apramycin (yellow, dark blue, and red), the RNA of the apramycin complex (pale blue and gray), and a fragment of the ribosomal protein S12 (green) from the 30S subunit structure are shown. The 3'-hydroxy group of the terminal aminoglycoside ring (III) clashes with the side chain of the T40 residue (green and dark blue, labeled) within S12.

that it plays a key role as a control element for translocation of the mRNA–tRNA complex during translation.<sup>[27]</sup> Apramycin binding to the decoding site might interfere with the local conformation of S12 around the T40 residue, a possibility suggesting a hypothesis for the unique inhibitory action of apramycin on ribosome translocation.<sup>[17]</sup> Further support for this hypothesis comes from genetic studies of apramycin-resistant mutants of *E. coli*, which identified two genomic loci that conferred resistance to the aminoglycoside, *aprA* and *aprB*, both of which were mapped in the neighborhood of ribosomal gene *rpsL* (S12).<sup>[28]</sup>

The crystal structure of the apramycin–decoding-site complex reveals the molecular basis for the bacterial-target specificity of the aminoglycoside antibiotic. A pseudo-base-pair interaction of the bicyclic sugar (II) with A1408 and alignment of the terminal sugar (III) with C1409–G1491 in a pseudo base triple are key determinants of the bacterial–RNA complex which cannot form with the eukaryotic target. If the *E. coli* numbering scheme is applied, the eukaryotic decoding site carries G1408 and A1491 substitutions (Figure 1 a), both of which would disrupt specific interactions with apramycin. In fact, the respective eukaryotic mutations, when introduced into the bacterial decoding site, confer resistance to apramycin.<sup>[20,26]</sup> Mass-spectrometric studies of aminoglycoside binding to RNA have produced somewhat contradictory results that suggest apramycin binds with comparable affinity to the wild-type bacterial decoding site and to A1408G mutants.<sup>[29]</sup> Crystallographic investigation of complexes between apramycin and eukaryotic decoding-site constructs indicates, however, that the aminoglycoside binds to the eukaryotic

RNA in a fashion very distinct from its binding to the bacterial target; it is buried entirely inside the deep groove of the eukaryotic RNA and is shifted down toward the lower flanking stem of the adenine internal loop.<sup>[30]</sup> The biological significance of this interaction is currently not known. Apramycin has recently been shown to also bind with nanomolar affinity to stem loop I (SLI) of bacterial RepA mRNA, thereby disrupting a pseudoknot interaction that regulates translation of the protein.<sup>[31]</sup> Interestingly, aminoglycosides of the 4,5- and 4,6-disubstituted 2-DOS classes do not bind to the mRNA stem loop. The SLI RNA secondary structure shares little similarity with either bacterial or eukaryotic decoding-site RNA, a fact suggesting that a different binding mode for apramycin might exist for each of these targets.

The three-dimensional structures of aminoglycoside–decoding-site complexes,<sup>[7,9–13]</sup> including the apramycin–RNA crystal structure described here, illustrate a paradigm of RNA recognition by natural products derived from 2-DOS. Namely, the 2-DOS moiety is positioned face-on in the deep groove of RNA and serves as an “RNA-friendly” anchor scaffold that bridges adjacent base pairs.<sup>[32,33]</sup> Branching out from the central 2-DOS anchor are glycoside substituents that provide additional target-specific contacts by pseudo-base-pair and -triple interactions. A similar concept of base-pair-like interactions of glycosides with nucleobases has been proposed previously by Wong and co-workers who recognized the potential of 1,3-hydroxyamine motifs found in aminoglycosides for hydrogen-bonding alignment with the Hoogsteen face of guanosine.<sup>[34]</sup> The apramycin complex with the bacterial decoding site represents the first example of glycoside pseudo base pairs and triples simultaneously participating in RNA-target recognition by a small molecule.

Binding of the apramycin 2-DOS moiety to the decoding-site RNA at a position that is nearly identical to the 2-DOS arrangement in complexes with 4,5- and 4,6-disubstituted aminoglycosides<sup>[10–12,14]</sup> suggests that novel ligands might be created by attaching additional sugar moieties at the 5- or 6-positions of apramycin (Figure 2 b,c). Indeed, the structural relationship between the 4-monosubstituted 2-DOS apramycin and aminoglycosides of the 4,5- and 4,6-disubstituted 2-DOS classes has been noted before and led to the synthesis of 6-*O*-(3-amino-3-deoxy- $\alpha$ -D-glucopyranosyl)apramycin (**2**, Scheme 1), an apramycin/tobramycin hybrid, and 5-*O*-( $\beta$ -D-ribofuranosyl)apramycin (**3**, Scheme 1), an apramycin/ribostamycin hybrid.<sup>[35]</sup> Microbiological testing in a range of organisms revealed a generally two- to fourfold increase in potency of the large aminoglycoside hybrids **2** and **3** over apramycin.<sup>[35]</sup> One exception was the test against *Pseudomonas aeruginosa*, where the potency of **2** and **3** was less than that of the parent compound, possibly due to poor permeability of the large molecules.

In the past, our group and others have used structural information from decoding-site complexes of aminoglycosides to design novel synthetic ligands for the bacterial target.<sup>[33,36,37]</sup> The structure of the apramycin–decoding-site complex lends support to a design strategy that we suggested earlier, which aims to exploit interactions in the shallow groove of decoding-site RNA, specifically with C1409.<sup>[37]</sup>



## Experimental Section

RNA crystallization was performed with gel-purified and desalted oligonucleotides purchased from Dharmacon Research (Lafayette, CO). RNA was annealed by heating in buffer (50 mM sodium cacodylate (pH 6.5), 3 mM magnesium chloride, 0.05 mM ethylenediaminetetraacetate (EDTA)) at 75 °C for 1 min and cooling to room temperature. Apramycin was purchased as the sulfate (Sigma, St. Louis, MO) and prepared as a 1.5 mM stock solution in buffer (200 mM sodium cacodylate (pH 6.5), 300 mM potassium chloride). For crystallization, 0.25 mM RNA in buffer (1.5  $\mu$ L), apramycin stock solution (1.5  $\mu$ L), and a solution of 2.5% 2-methyl-2,4-pentanediol (MPD) and 2.5% glycerol in water (1.5  $\mu$ L) were mixed and equilibrated against 65–80% MPD for hanging-drop vapor diffusion. Crystal plates of the apramycin–RNA complex grew within three days at 37 °C. For X-ray diffraction, crystals were flash-cooled in liquid nitrogen and transferred to a cold N<sub>2</sub> stream. Data sets were collected on beamline 14IDB at the Advanced Photon Source (APS) at Argonne National Laboratory (Argonne, IL). The crystals of the space group *P*<sub>2</sub><sub>1</sub><sub>2</sub><sub>1</sub> diffracted to 2.7 Å resolution. Data were processed with the DENZO/SCALEPACK software.<sup>[38]</sup> Structures were solved by molecular replacement by using a published decoding-site RNA structure<sup>[10]</sup> as the initial model with the AMORE program<sup>[39]</sup> and were refined to *R*/*R*<sub>free</sub> values of 0.24/0.30 with the CNX/CNS program (Accelrys, San Diego, CA).<sup>[40]</sup> For complete crystal data and refinement statistics, see the Supporting Information. Coordinates and structure factors have been deposited in the Protein Data Bank (accession code: 1YRJ).

Received: January 5, 2005

Published online: April 6, 2005

**Keywords:** antibiotics · glycosides · molecular recognition · RNA · structure–activity relationships

- [1] C. Walsh, *Antibiotics: Actions, Origins, Resistance*, ASM Press, Washington, DC, 2003.
- [2] T. Hermann, *Biopolymers* 2003, 70, 4–18.
- [3] T. Auerbach, A. Bashan, J. Harms, F. Schluenzen, R. Zarivach, H. Bartels, I. Agmon, M. Kessler, F. Pioletti, F. Franceschi, A. Yonath, *Curr. Drug Targets Infect. Disord.* 2002, 2, 169–186.
- [4] D. Moazed, H. F. Noller, *Nature* 1987, 327, 389–394.
- [5] J. Woodcock, D. Moazed, M. Cannon, J. Davies, H. F. Noller, *EMBO J.* 1991, 10, 3099–3103.
- [6] a) T. Hermann, *Angew. Chem.* 2000, 112, 1962–1979; *Angew. Chem. Int. Ed.* 2000, 39, 1890–1904; b) T. Hermann, Y. Tor, *Expert Opin. Ther. Pat.* 2005, 15, 49–62; c) Q. Vicens, E. Westhof, *ChemBioChem* 2003, 4, 1018–1023.
- [7] J. M. Ogle, D. E. Brodersen, W. M. Clemons, M. J. Tarry, A. P. Carter, V. Ramakrishnan, *Science* 2001, 292, 897–902.
- [8] a) J. M. Ogle, A. P. Carter, V. Ramakrishnan, *Trends Biochem. Sci.* 2003, 28, 259–266; b) J. M. Ogle, F. V. Murphy, M. J. Tarry, A. P. Carter, V. Ramakrishnan, *Cell* 2002, 111, 721–732.
- [9] A. P. Carter, W. M. Clemons, D. E. Brodersen, R. J. Morgan-Warren, B. T. Wimberly, V. Ramakrishnan, *Nature* 2000, 407, 340–348.
- [10] Q. Vicens, E. Westhof, *Structure* 2001, 9, 647–658.
- [11] Q. Vicens, E. Westhof, *Chem. Biol.* 2002, 9, 747–755.
- [12] Q. Vicens, E. Westhof, *J. Mol. Biol.* 2003, 326, 1175–1188.
- [13] a) D. Fourmy, M. I. Recht, S. C. Blanchard, J. D. Puglisi, *Science* 1996, 274, 1367–1371; b) S. Yoshizawa, D. Fourmy, J. D. Puglisi, *EMBO J.* 1998, 17, 6437–6448.
- [14] Q. Vicens, E. Westhof, *Biopolymers* 2003, 70, 42–57.
- [15] S. O'Connor, L. K. Lam, N. D. Jones, M. O. Chaney, *J. Org. Chem.* 1976, 41, 2087–2092.
- [16] a) R. Ryden, B. J. Moore, *J. Antimicrob. Chemother.* 1977, 3, 609–613; b) J. R. Walton, *J. Antimicrob. Chemother.* 1978, 4, 309–313.
- [17] S. Perzynski, M. Cannon, E. Cundliffe, S. B. Chahwala, J. Davies, *Eur. J. Biochem.* 1979, 99, 623–628.
- [18] P. Pfister, S. Hobbie, Q. Vicens, E. C. Böttger, E. Westhof, *ChemBioChem* 2003, 4, 1078–1088.
- [19] M. I. Recht, J. D. Puglisi, *Antimicrob. Agents Chemother.* 2001, 45, 2414–2419.
- [20] M. I. Recht, S. Douthwaite, J. D. Puglisi, *EMBO J.* 1999, 18, 3133–3138.
- [21] a) P. A. Skeggs, J. Thompson, E. Cundliffe, *Mol. Gen. Genet.* 1985, 200, 415–421; b) A. A. Beauclerk, E. Cundliffe, *J. Mol. Biol.* 1987, 193, 661–671.
- [22] N. Ban, P. Nissen, J. Hansen, P. B. Moore, T. A. Steitz, *Science* 2000, 289, 905–920.
- [23] a) B. T. Wimberly, R. Guymon, J. P. McCutcheon, S. W. White, V. Ramakrishnan, *Cell* 1999, 97, 491–502; b) G. L. Conn, D. E. Draper, E. E. Lattman, A. G. Gittis, *Science* 1999, 284, 1171–1174.
- [24] a) D. J. Klein, P. B. Moore, T. A. Steitz, *J. Mol. Biol.* 2004, 340, 141–177; b) A. C. Cheng, W. W. Chen, C. N. Fuhrmann, A. D. Frankel, *J. Mol. Biol.* 2003, 327, 781–796; c) T. Hermann, E. Westhof, *Chem. Biol.* 1999, 6, 335–343.
- [25] Biological activities: IC<sub>50</sub> values of in vitro translation inhibition: 0.2  $\mu$ M apramycin, 1.8  $\mu$ M aprosamine; minimum inhibitory concentrations (MICs) against a standard *Escherichia coli* strain: 2  $\mu$ g mL<sup>-1</sup> of apramycin, 32  $\mu$ g mL<sup>-1</sup> of aprosamine. Assays were performed as described in: S. Barluenga, K. B. Simonsen, E. S. Littlefield, B. K. Ayida, D. Vourloumis, G. C. Winters, M. Takahashi, S. Shandrick, Q. Zhao, Q. Han, T. Hermann, *Bioorg. Med. Chem. Lett.* 2004, 14, 713–718.
- [26] E. A. DeStasio, A. E. Dahlberg, *J. Mol. Biol.* 1990, 212, 127–133.
- [27] A. R. Cukras, D. R. Southworth, J. L. Brunelle, G. M. Culver, R. Green, *Mol. Cell* 2003, 12, 321–328.
- [28] B. Vasiljevic, D. Fira, L. Topisirovic, *J. Basic Microbiol.* 1993, 3, 47–51.
- [29] R. H. Griffey, S. A. Hofstadler, K. A. Sannes-Lowery, D. J. Ecker, S. T. Croke, *Proc. Natl. Acad. Sci. USA* 1999, 96, 10129–10133.
- [30] T. Hermann, unpublished results.
- [31] J. C. B. DeNap, J. R. Thomas, D. J. Musk, P. J. Hergenrother, *J. Am. Chem. Soc.* 2004, 126, 15402–15404.
- [32] a) Y. Tor, T. Hermann, E. Westhof, *Chem. Biol.* 1998, 5, 277–283; b) S. J. Sucheck, Y.-K. Shue, *Curr. Opin. Drug Discovery Dev.* 2001, 4, 462–470; c) S. Yoshizawa, D. Fourmy, R. G. Eason, J. D. Puglisi, *Biochemistry* 2002, 41, 6263–6270.
- [33] D. Vourloumis, M. Takahashi, G. C. Winters, K. B. Simonsen, B. K. Ayida, S. Barluenga, S. Qamar, S. Shandrick, Q. Zhao, T. Hermann, *Bioorg. Med. Chem. Lett.* 2002, 12, 3367–3372.
- [34] a) M. Hendrix, P. B. Alper, E. S. Priestley, C.-H. Wong, *Angew. Chem.* 1997, 109, 119–122; *Angew. Chem. Int. Ed. Engl.* 1997, 36, 95–98; b) C.-H. Wong, M. Hendrix, D. D. Manning, C. Rosenbohm, W. A. Greenberg, *J. Am. Chem. Soc.* 1998, 120, 8319–8327.
- [35] Y. Abe, S. Nakagawa, T. Naito, H. Kawaguchi, *J. Antibiot.* 1981, 34, 1434–1446.
- [36] a) P. Alper, M. Hendrix, P. Sears, C.-H. Wong, *J. Am. Chem. Soc.* 1998, 120, 1965–1978; b) J. Haddad, L. P. Kotra, B. Llano-Sotelo, C. Kim, E. F. Azucena, M. Liu, S. B. Vakulenko, C. S. Chow, S. Mobashery, *J. Am. Chem. Soc.* 2002, 124, 3229–3237; c) D. Vourloumis, G. C. Winters, M. Takahashi, K. B. Simonsen, B. K. Ayida, S. Shandrick, Q. Zhao, T. Hermann, *ChemBioChem* 2003, 4, 879–885; d) K. B. Simonsen, B. K. Ayida, D. Vourloumis, G. C. Winters, M. Takahashi, S. Shandrick, Q. Zhao, T. Hermann, *ChemBioChem* 2003, 4, 886–890; e) D. Vourloumis,

- G. C. Winters, K. B. Simonsen, M. Takahashi, B. K. Ayida, S. Shandrick, Q. Zhao, Q. Han, T. Hermann, *ChemBioChem* **2005**, *6*, 58–65.
- [37] K. B. Simonsen, B. K. Ayida, D. Vourloumis, M. Takahashi, G. C. Winters, S. Barluenga, S. Qamar, S. Shandrick, Q. Zhao, T. Hermann, *ChemBioChem* **2002**, *3*, 1223–1228.
- [38] Z. Otwinowski, W. Minor, *Methods Enzymol.* **1997**, *276*, 307–326.
- [39] J. Navaza, *Acta Crystallogr. Sect. A* **1994**, *50*, 157–163.
- [40] A. T. Brünger, P. D. Adams, G. M. Clore, W. L. DeLano, P. Gros, R. W. Grosse-Kunstleve, J.-S. Jiang, J. Kuszewski, M. Niges, N. S. Pannu, R. J. Read, L. M. Rice, T. Simonson, K. L. Warren, *Acta Crystallogr. Sect. D* **1998**, *54*, 905–921.